UNIVERSITÀ DEGLI STUDI DI TORINO

An insulin-like growth factor-II intronic variant affects local DNA conformation and ovarian cancer survival

Lingeng Lu[1,2,*], Evan Risch[1,†], Qian Deng[1,3,†], Nicoletta Biglia[4], Elisa Picardo[5], Dionyssios Katsaros[5] and Herbert Yu[1,2,6]

1 Department of Chronic Disease Epidemiology, Yale School of Public Health and
2 Yale Cancer Center, New Haven, CT 06520-8034, USA,
3 National Center for Chronic and Non-communicable Disease Control and Prevention, Chinese Center for Disease Control and Prevention, Beijing 102206, China,
4 Division of Gynecology, Mauriziano Hospital, 10126 Turin, Italy and
5 Department of Gynecologic Oncology, Azienda Ospedaliera OIRM-S. ANNA and University of Turin, 10126 Turin, Italy
6 Present address: Cancer Epidemiology Program, University of Hawaii Cancer Center, Honolulu, HI 96813, USA
*To whom correspondence should be addressed. Department of Chronic Disease Epidemiology, Yale School of Public Health, Yale University, 60 College Street, New Haven, CT 06520-8034, USA. Tel: +1 203 737 6812; Fax: +1 203 785 2207;
Email: lingeng.lu@yale.edu

Summary: Insulin-like growth factor-II (IGF-II) may be a prognostic marker in ovarian cancer, and its intronic single nucleotide polymorphism (SNP) rs4320932 has been associated with risk of the disease. We determined whether rs4320932 is associated with IGF-II expression and patient survival in ovarian cancer, and explored whether the SNP variation affects DNA conformation both in the absence of and presence of carboplatin. IGF-II genotype (rs4320932) and phenotype were analyzed in 212 primary invasive epithelial ovarian cancer tissue samples with Taqman® SNP genotyping assays, quantitative reverse transcription–polymerase chain reaction and commercial enzyme-linked immunosorbent assay. DNA conformation was evaluated by circular dichroism (CD) spectra. Kaplan–Meier survival curves and Cox proportional hazard regression models were used to analyze the SNP associations with patient survival. The C allele of rs4320932, previously associated with decreased risk of ovarian cancer development, was here associated with significantly elevated risks of relapse (*P*trend = 0.0002) and death (*P*trend = 0.0006), remaining significant in multivariate analyses. The adjusted hazard ratios were 3.05 (95% confidence interval [CI]: 1.47–6.37) for relapse and 3.28 (95% CI: 1.64–6.57) for death, respectively. The variant was also significantly associated with chemotherapy response, but not with other clinicopathologic variables or with IGF-II expression. DNA with genotypes TT and CC had distinct CD spectra in both the absence of and presence of carboplatin. These findings suggest that the intronic SNP rs4320932 affects patient survival and chemotherapy response via alteration of DNA conformation, but not through regulation of IGF-II expression. This novel finding may have implications in individualized medicine for the design of specific molecules targeting DNA of specific conformations.

Introduction Insulin-like growth factor-II (IGF-II) is a mitogenic peptide and plays important roles in the regulation of cellular proliferation, differentiation and embryonic development in both autocrine and paracrine manners (1). The human IGF-II gene is located on the short arm of chromosome 11 (11p15.5) and spans approximately 30 kb in length. The gene consists of 10 exons and 4 promoters (labeled P1–P4), each promoter driving distinct transcription, producing promoter-specific transcripts with unique 5′-untranslated regions. The different promoter-

specific transcripts share a common translated region based on exons 8, 9 and part of exon 10 (2). IGF-II precursors are post-translationally processed to mature peptides, which function as ligands of type I IGF receptors, activating IGF signal pathways. Evidence suggests that IGF-II is involved in neoplastic transformation and tumor progression of breast, prostate, bladder, colon, gastric and ovarian cancers (3–6). Utilization of antibody-blocking IGF signaling is under clinical trial for targeted cancer treatment. Higher IGF-II expression is seen in ovarian cancer compared with normal ovarian tissue, and IGF-II expression is positively associated with risk of ovarian cancer and with poor prognosis (7–10). We have also reported that high IGF-II promoter-specific transcripts, particularly P3 and P4, are associated with unfavorable prognosis in ovarian cancer (2). Studies have shown that certain women are genetically susceptible to ovarian cancer. High penetrance mutations in *BRCA1* and *BRCA2* occur in about 10–15% of cases (11). Efforts have been made to identify single nucleotide polymorphisms (SNPs) associated with ovarian cancer risk (12). Recently, from analysis of tag SNPs in the IGF genes, an intronic SNP (rs4320932) of IGF-II was associated with ovarian cancer risk (13). Although it is possible that the SNP may be a driver or modifier of IGF network signaling, the underlying molecular mechanisms of the genetic association remain poorly characterized, and it is yet to be known whether or not the SNP can be utilized as a potential marker for prognosis and individualized care in ovarian cancer. DNA secondary structure in its double helix conformation has important biological relevance in the physiological processes of cell proliferation and apoptosis. DNA conformation can affect the recognition and binding of proteins and small ligand molecules (14–16), thereby influencing DNA replication, damage repair and apoptosis. DNA sequences and microenvironments are two important determinants in local and global DNA conformation (17). Under normal physiological conditions, double-stranded DNA constitutes a right-hand B-form double helix (17). Ethanol shifts DNA to adopt a right-hand A-form (frequently observed in RNA molecules) in a more compact helical structure (18,19), whereas the transition from B-form to left-hand Z-form can occur under certain conditions such as high salt concentration (17,20). Cisplatin/carboplatin is a widely used platinum-based chemotherapeutic agent in the management of human cancer. Antitumor properties of platinum-based agents involve the inhibition of DNA replication and the activation of apoptosis signal pathways through binding to DNA to form intra- or interstrand crosslinks with adjacent guanine or adenine bases (21,22). The crosslinks cause helical structural distortions and the destruction of nucleotide base parallel stacking at platination sites (22–24). However, few studies have reported whether or not SNPs affect cisplatin/ carboplatin-induced alterations of DNA conformation. Thus, the purposes of this study were to investigate in ovarian cancer the associations of IGF-II genotype (rs4320932) with patient survival and with the expression of IGF-II, and to explore whether rs4320932 modifies alterations in DNA conformation caused by carboplatin.

Materials and methods *Study patients* Between October 1991 and February 2000, a clinical study was conducted in the Gynecologic Oncology Unit at University of Turin in Italy. Subsequent to university institutional review board approval, fresh tumor samples were collected from 212 patients undergoing surgery for primary invasive epithelial ovarian cancer. The specimens were snap frozen in liquid nitrogen immediately after resection, and then transferred to a −80□C freezer for long-term storage until analysis. Patient clinical and pathology information was obtained from the medical charts and pathology reports. The average age of patients at surgery was 57.7 years (range: 26–82). Of the 212 patients, 34 (16.0%) had grade 1, 40 (18.9%) had grade 2 and 137 (64.6%) had grade 3 tumors. Based on the criteria of the International Federation of Gynecology and Obstetrics Classification (25), disease stages I–IV were found in 52 (24.5%), 12 (5.7%), 133 (62.7%) and 14 (6.6%) patients, respectively. The most common histology was papillary serous carcinoma (40.1%), followed by endometrioid (19.3%), undifferentiated (17.5%), mucinous

(8.5%), clear cell (7.6%), mullerian (6.6%) and other (0.5%) according to the World Health Organization guidelines (26). After cytoreduction surgery, patients were followed through June 2001. The median follow-up time was 31 months, ranging from 0.6 to 114 months. Of the 212 patients, 178 received standard post-operative platinum-based chemotherapy, one had chemotherapy without platinum and 33 did not receive chemotherapy due to early stage disease, progressive tumor behavior, advanced patient age or severe comorbidity. Each patient was evaluated for treatment response based on clinical examination, computed tomography scan and CA-125, which was classified into four categories: (i) complete response, resolution of all evidence of disease for at least 1 month after the last cycle of chemotherapy; (ii) partial response, a decrease of ≥50% in the product of the diameters (maximum and minimum) of all measurable lesions without the development of new lesions for at least 1 month; (iii) stable disease, a decrease of <50% or an increase of <25% in the product of the diameters of all measurable lesions and (iv) progressive disease, an increase of ≥25% in the product of the diameters of all measurable lesions or the development of new lesions. Of the 176 patients who had information on response to platinum-based chemotherapy, the 128 (72.7%) patients who had complete response were considered 'responders' in our data analyses, whereas the 48 (27.3%) patients in the other three categories (partial response, stable disease and progressive disease) were grouped as 'non-responders'. *Genomic DNA extraction and IGF-II SNP genotyping* Fresh-frozen dissected tumor specimens, which, examined by two independent pathologists, contained 80–90% tumor cells, were pulverized manually in liquid nitrogen. Genomic DNA was extracted from approximately 100 mg of tissue powder using a standard phenol–chloroform protocol, and the quality and quantity of the extracted DNA samples were determined spectrophotometrically. Genotyping of the IGF-II SNP (rs4320932) was performed using the Taqman□ SNP genotyping assay (Applied Biosystems, Foster City, CA) following the manufacturer's instructions. Briefly, in a volume of 8 µl PCR reaction, 4 µl of 2□ iTaq™ Fast Supermix with ROX (Bio-Rad, Hercules, CA) was mixed with pre-designed Taqman□ primers/probes (Applied Biosystems), approximately 10–50 ng of genomic DNA, and distilled water. The PCR conditions were initial denaturing at 95□C for 10 min followed by 50 cycles of denaturing at 92□C for 15 s and annealing/extension at 60□C for 1 min. The reactions were carried out in an ABI 7500 Real-time PCR System (Applied Biosystems). Ten percent of samples were run in duplicate for quality control, with 100% concordance. *Analysis of IGF messenger RNA levels and peptides* Fresh-frozen dissected tumor specimens, which, examined by two independent pathologists, contained 80–90% tumor cells, were pulverized manually in liquid nitrogen for extraction of total RNA. The quality of ribonuclease-free deoxyribonuclease-treated total RNA was determined using 1% agarose gel electrophoresis for the integrity of 18s and 28s ribosomal RNA. The messenger RNA (mRNA) levels of IGF-II and promoter-specific transcripts of the IGF-II gene were evaluated using SYBR□ green-based real-time PCR as reported previously (2,10). The quantitative PCR was performed in the Chromo4TM Real-time PCR System (MJ Research, Waltham, MA). Briefly, in a 20 µl of PCR reaction volume, 1 µl of complementary DNA template was mixed with 10 µl of 2□ Power SYBR□ PCR master mix (Applied Biosystems), 200 nM of paired primers of either target gene or glyceraldehyde 3-phosphate dehydrogenase as an internal control and distilled water. The PCR amplification included initial incubation at 50□C for 2 min, denaturing at 95□C for 10 min, 40 cycles of denaturing at 95□C for 15 s and annealing at 60□C for 1 min. Melting curves were analyzed after each run to verify the size of the PCR product. Each sample was analyzed in duplicate, and the analysis was repeated for samples with CV over 5%. Tissue levels of IGF-II peptides were evaluated using a commercial Enzyme- Linked Immunosorbent Assay Kit (Diagnostic Laboratories Systems, Webster, TX) following the manufacturer's directions. To adjust for the amount of tissue used for protein extraction, we measured the concentration of total protein in each specimen using the bicinchoninic acid method (Pierce, Rockford, IL).

Preparation of double-stranded DNA amplicons A set of primers complementary to the upstream and downstream sequences of the SNP rs4320932 (T/C) was designed. The sequences of the forward and reverse primers were 5′-CAA CAC ATG CCA GAT TTG AAT C and 5′-CCT GTG TTG GGA TTT AAT TGT C, respectively. PCR reactions were performed using 2× HotstarTaq® master mix (Qiagen, Valencia, CA), with primers each in final concentration of 200 nM, and genomic DNA templates extracted from individuals with either homozygous wild-type (TT) or variant (CC) genotypes. The PCR thermal conditions consisted of initial activation at 95°C for 15 min, 40 cycles of denaturation at 95°C for 30 s, annealing at 55°C for 30 s and extension at 72°C for 1 min. A final extension was performed at 72°C for 10 min. The PCR procedure amplified 160 bp products that were then isolated through agarose gel electrophoresis and purified with the Qiaquick® Gel Extraction Kit (Qiagen) according to the manufacturer's protocol, and the purified products were used as templates for sequencing at the Yale University Keck Core Sequencing Facility to confirm their sequence identities, as well as for conformation analysis. The amount of purified PCR product was determined with a NanoDrop® spectrophotometer (NanoDrop Technologies, Wilmington, DE). *Circular dichroism spectroscopy and DNA secondary structure comparison* Using circular dichroism (CD) spectroscopy as described previously (27), we compared experimentally the DNA secondary structures between the purified PCR products carrying the homozygous wild-type genotype versus the variant one so that we could differentiate the alterations of DNA structure due to the SNP. The denatured oligonucleotides (~82 ng/μl in 10 mM Tris–HCl buffer, pH 8.5), in duplicate for each genotype, were annealed for 1 h at 37°C, followed by incubation overnight at 37°C in the absence or presence of carboplatin (equal molar ratio of DNA to carboplatin; 0.8 μl of 0.27 nmol/μl carboplatin in dimethyl sulfoxide was added). The incubated DNA oligos were analyzed with a ChirascanTM CD spectrometer (Applied Photophysics, Surrey, UK). The CD spectra in wavelengths ranging from 220 to 310 nm were acquired at 6°C in 1.00 mm Quartz cuvettes with bandwidth of 0.5 nm and 0.9 s of time per point. Each sample was run three times to obtain the CD spectra in millidegrees (ellipticity), which was adjusted with the CD spectrum of the Tris–HCl (10 mM) buffer alone as a blank control (there was no difference in CD spectra in the wavelengths ranging from 220 to 310 nm between the buffer alone and buffer plus dimethyl sulfoxide [~0.4%, v/v]). The average and standard deviation per sample was calculated based on six measurements. Graphs of the CD spectra show ellipticity (θ) as a function of wavelength (λ). The positions of peaks and the curve shape represent conformations of double-stranded DNA. The B-form CD spectrum, characterized by a positive peak between 260 and 280 nm, and a negative peak between 240 and 250 nm, is the most frequently observed CD spectrum for a typical double-stranded DNA molecule (17). The position and intensity (ellipticity, which is proportional to the difference between absorbance of left circularly polarized and right circular polarized light) of peaks are associated with chromophores (bases) and conformational properties (α-helix rotation and the number of base pairs per turn) (17,28). *Statistical analysis* Expression index was calculated for the expression of a target gene using the formula: 1000 × 2(−ΔCt), where ΔCt = Ct (IGF-II) – Ct (glyceraldehyde 3-phosphate dehydrogenase). Chi-square tests or Fisher exact tests were used to determine the associations between the IGF-II SNP genotype and clinical and pathologic variables. Survival analysis was performed to assess the association of IGF-II genotype with risk of disease progression and mortality using Cox proportional hazards regression models and Kaplan–Meier survival curves. Wilcoxon rank sum tests were carried out to analyze *cis*-acting regulatory expression quantitative trait loci (eQTL) in IGF-II based on the SNP expression data. All statistical analyses were performed using SAS version 9.2 (SAS Institute, Cary, NC). All *P*-values are two-sided. The bold values in tables are statistically significant ($P < 0.05$).

Results *Associations of IGF-II genotype with disease characteristics* Table I presents the associations between *IGF-II* (rs4320932) genotype and ovarian cancer characteristics. Therein, we observe no associations between rs4320932 genotype and either disease stage, tumor grade or histologic type. A lack of association was also seen with debulking result and residual tumor size. However, the SNP genotype was significantly associated with response to chemotherapy (*P*trend = 0.028). In patients who had complete response to chemotherapy, only 3.1% (*n* = 4) were found to have CC genotype, whereas in patients who did not so respond, CC genotype frequency was 16.7%. The significant association between the genotype and response to chemotherapy remained in the subgroup of patients who had residual tumor (*P* = 0.014 and *P*trend = 0.017; data not shown). *Associations of IGF-II genotype with patient survival* Kaplan–Meier survival curves showed that patients with the wild-type genotype (TT) had better survival than those with variant genotypes (*P* < 0.0001 for overall survival and *P* = 0.0004 for disease progression- free survival, respectively; Figure 1A and B). The median overall survivals were 68.9 months (95% confidence interval [CI]: 46.6–∞), 40.2 months (95% CI: 32.7–∞) and 18.5 months (95% CI: 7.3–30.1) for TT, TC and CC, respectively. Patients with wild-type TT and variant TC and CC genotypes had median progression-free survivals of 72.0 months (95% CI: 32.6–∞), 24.2 months (95% CI: 14.8–44.1) and 11.9 months (95% CI: 7.8–21.0), respectively. To adjust for potential confounding of patient age at surgery, disease stage, tumor grade, residual tumor size and histological type on the SNP associations with survival, we performed multivariate Cox proportional hazard regression analysis (Table II). Compared with patients with TT genotype, those with TC and CC genotypes had higher adjusted mortality hazard ratios (adj-HRs), 1.48 (95% CI: 0.94–2.34) and 3.28 (95% CI: 1.64–6.57), respectively. The trend in risk was significant (*P* = 0.001). Similarly, patients with genotypes TC and CC had higher risks of relapse than those with TT: adj-HRs 1.76 (95% CI: 1.14–2.71) and 3.05 (95% CI: 1.47–6.37), respectively (*P*trend = 0.0004). We also analyzed the genotype association with survival according to the dominant model. Significantly increased risks of relapse and death were observed for the variant genotypes (TC/CC); the adj-HRs were 1.92 (95% CI: 1.28–2.88) and 1.74 (95% CI: 1.15–2.65), respectively. *Associations of IGF-II genotype and expression* Table III presents the medians and ranges (5th–95th) of expression of IGF-II total, and P1, P2, P3 and P4. No significant associations were found between genotype and IGF-II expression or promoter-specific transcripts. *Effects of rs4320932 and carboplatin on local DNA secondary structure* CD analyses showed that in the absence of carboplatin, both wildtype (TT) and variant (CC) DNA had the typical B-form CD spectrum but differed in maximum intensity by a 1.5 nm shift in the maximal CD wavelength (Figure 2A). Genotype TT had a positive maximum intensity (mean = 2.18 mdeg, standard error of mean [SEM] = 0.026 mdeg) at wavelength 274.5 nm, whereas variant CC had a maximum intensity (mean = 1.89 mdeg, SEM = 0.039 mdeg) at wavelength 276 nm. The difference in maximum intensity is statistically significant (*P* = 8.6 □ 10−5). Both genotypes had negative peaks at wavelength 245 nm. The TT form had a statistically significant deeper negative peak (mean = −2.52 mdeg, SEM = 0.088 mdeg) compared with CC (mean = −2.26 mdeg, SEM = 0.070 mdeg; *P* = 0.041). The CD spectra also showed that carboplatin caused alleledependent alterations in DNA conformation. Carboplatin treatment led to a reduction in maximum intensity and the appearance of positive shoulders in both genotypes (Figure 2B and C); however, different positions of the shoulders were found according to SNP genotype. For the carboplatin-treated DNA with genotype CC, the intensity of one shoulder at wavelength 276 nm (mean = 1.88 mdeg, SEM = 0.062 mdeg) was not significantly different (*P* = 0.96), whereas the intensity of another at wavelength of 279.5 nm (mean = 1.69 mdeg, SEM = 0.048 mdeg) was significantly lower than the maximum intensity of the naive (untreated) DNA (*P* = 0.010). Moreover, we also found a significant reduction of the minimal intensity (mean = −2.49 mdeg, SEM = 0.058 mdeg) at wavelength 242.5 nm (a 2.5 nm shift) for the carboplatin-treated genotype CC DNA compared with

the naive DNA (P = 0.026; Figure 2B). For the drug-treated DNA carrying genotype TT, one shoulder was located at wavelength 282.5 nm (mean intensity = 1.89 mdeg, SEM = 0.058 mdeg) and another at 274.5 nm (mean intensity = 1.99 mdeg, SEM = 0.067 mdeg; Figure 2C). Compared with the maximum intensity of the naive DNA, the intensities of the two shoulders in the carboplatin-treated TT genotype DNA were significantly lower (P = 0.001 and P = 0.023, respectively). Although the minimal intensity (mean = −2.66 mdeg, SEM = 0.065 mdeg) at the negative band was smaller for the carboplatin-treated genotype TT DNA than for the naive DNA, the difference was not statistically significant (P = 0.22). Additionally, the minimal intensity remained at wavelength 245 nm.

Discussion In this study, we demonstrated that the intronic SNP rs4320932 in the IGF-II gene was associated with patient survival in epithelial ovarian cancer. Patients carrying variant genotypes of rs4320932 had higher risks of relapse and death; the associations were independent of other prognostic indicators including patient age at surgery, disease stage, tumor grade, histologic type and residual tumor size. To our knowledge, this is the first study to show an IGF-II SNP potentially involved in the prognosis of ovarian cancer. Interestingly, the direction of the SNP association with relapse and death was opposite to the direction of the genotype association with ovarian cancer risk. Pearce *et al.* (13) reported that the rs4320932 variant was a protective factor for ovarian cancer in their twophase case-control study. This discrepancy suggests that the rs4320932 variant may play different roles in cell transformation and tumor progression. In tumorigenesis, rs4320932 may be a passenger rather than a driver because rs4320932 is an intronic SNP, not located in the predicted regulation regions of IGF-II transcription, based on genome browser data (http://genome.ucsc.edu; data not shown). It has been reported that IGF-II expression is associated with the sensitivity of cancer cells to platinum drugs. Overexpression of IGF-II leads to cell resistance to platinum agents (29–31). In this study, we found that the SNP rs4320932 of IGF-II was associated with chemotherapy response: patients with genotype CC had worse response to chemotherapy than those with genotype TT. However, our eQTL analyses did not show a significant association of rs4320932 with IGF-II expression. These findings prompted us to ask whether or not different response to platinum-based chemotherapy between two genotypes could be due to different DNA conformations. Indeed, we found different CD spectra between genotype TT and CC DNAs, suggesting that the two genotypes may have different DNA conformations. This difference in conformation may affect the binding of chiral drugs and formation of crosslinks. One possibility is that the TT genotype has a more favorable DNA conformation to facilitate the binding of carboplatin and paclitaxel, both of which are chiral molecules. Several studies have reported that different DNA conformations can interfere with the binding of paclitaxel, thereby affecting its actions (32–34). Zhao *et al.* (35) also reported that chiral compounds target DNA in both a sequence- and conformation-specific manner. Furthermore, we found that carboplatin can induce alterations of DNA conformation, distorting DNA structures (helical bend and base stacking, as well as major groove in which protein binding sites are usually located) due to the formation of intra- and inter-strand crosslinks (22,36,37). Interestingly, the alterations of CD spectra are different between genotypes TT and CC, suggesting the structural alterations may be SNP dependent. This difference in structure caused by drug binding and SNP genotype may further affect recognition and binding of other regulatory proteins or molecules, thereby influencing the processes of DNA replication and repair, as well as cell apoptosis. One structure may have a higher affinity for the binding of proteins to DNA than the other, thereby affecting downstream biological processes. This assumption is supported by the findings in the Kim study (38), which showed that a single C-G transversion can cause the alteration of binding affinity of proteins to DNA. In this study, we did not find statistically significant association between the

genotype of rs4320932 and IGF-II expression. This finding is consistent with the eQTL result obtained in lymphoblastoid (LCLs) and NCI-60 cell lines in the SCAN database (http://www.scandb.org/newinterface/about.html) (39), suggesting it is not likely that the lack of association between rs4320932 and IGF-II expression is due to mask by the heterogeneity of tumor tissues in this study. We searched tagSNP in the region of 200 kb surrounding the SNP rs4320932 using HAPMAP (http://hapmap.ncbi.nlm. nih.gov); neither tagSNPs for rs4320932 nor this SNP as a tag for other SNPs were found when we chose 0.05 or higher as the minor allele frequency and 0.8 or higher as the tagger pairwise R-square. This suggests that based on the current knowledge, rs4320932 may not have any tagSNPs affecting IGF-II expression. Because this is a single institute study with a relatively small sample size, the findings of this study need further validation in independent studies with large sample size. In summary, the results in this study have shown the variant of rs4320932 to be associated with elevated risks of disease progression and death in epithelial ovarian cancer, and that patients with wild-type alleles have better response to chemotherapy than those with variant alleles. Additionally, eQTL analyses did not show associations with IGF-II expression. However, different DNA conformations were found in the region surrounding rs4320932 according to genotypes TT and CC in the absence and presence of carboplatin. These findings suggest that rs4320932 is a potential prognostic marker in epithelial ovarian cancer, and that the variation of rs4320932 in IGF-II may affect local DNA conformation, thereby modulating the effect of chemotherapy.

Funding The Honorable Tina Brozman Foundation (to L.L.).

Acknowledgements We thank Drs E.Gamazon and E.Dolan at University of Chicago for their discussion in writing this manuscript. We also thank Dr S.T.Mayne and the Honorable Tina Brozman Foundation committee for their supports in the project. *Conflict of Interest Statement:* None declared.

References

1. Toretsky,J.A. *et al.* (1996) Involvement of IGF-II in human cancer. *J. Endocrinol*., **149**, 367–372.
2. Lu,L. *et al.* (2006) Promoter-specific transcription of insulin-like growth factor-II in epithelial ovarian cancer. *Gynecol. Oncol*., **103**, 990–995.
3. Freier,S. *et al.* (1999) Expression of the insulin-like growth factors and their receptors in adenocarcinoma of the colon. *Gut*, **44**, 704–708.
4. Li,S.L. *et al.* (1998) Expression of insulin-like growth factor (IGF)-II in human prostate, breast, bladder, and paraganglioma tumors. *Cell Tissue Res*., **291**, 469–479.
5. Shiraishi,T. *et al.* (1998) Expression of insulin-like growth factor 2 mRNA in human gastric cancer. *Int. J. Oncol*., **13**, 519–523.
6. van Roozendaal,C.E. *et al.* (1998) Loss of imprinting of IGF2 and not H19 in breast cancer, adjacent normal tissue and derived fibroblast cultures. *FEBS Lett*., **437**, 107–111.
7. Sawiris,G.P. *et al.* (2002) Development of a highly specialized cDNA array for the study and diagnosis of epithelial ovarian cancer. *Cancer Res*., **62**, 2923–2928.
8. Yun,K. *et al.* (1996) Monoallelic expression of the insulin-like growth factor- 2 gene in ovarian cancer. *Am. J. Pathol*., **148**, 1081–1087.
9. Sayer,R.A. *et al.* (2005) High insulin-like growth factor-2 (IGF-2) gene expression is an independent predictor of poor survival for patients with advanced stage serous epithelial ovarian cancer. *Gynecol. Oncol*., **96**, 355–361.

10. Lu,L. *et al.* (2006) The relationship of insulin-like growth factor-II, insulinlike growth factor binding protein-3, and estrogen receptor-alpha expression to disease progression in epithelial ovarian cancer. *Clin. Cancer Res*., **12**, 1208–1214.
11. Risch,H.A. *et al.* (2006) Population BRCA1 and BRCA2 mutation frequencies and cancer penetrances: a kin-cohort study in Ontario, Canada. *J. Natl Cancer Inst*., **98**, 1694–1706.
12. Pharoah,P.D. *et al.* (2013) GWAS meta-analysis and replication identifies three new susceptibility loci for ovarian cancer. *Nat. Genet.*, **45**, 362–370.
13. Pearce,C.L. *et al.* (2011) Genetic variation in insulin-like growth factor 2 may play a role in ovarian cancer risk. *Hum. Mol. Genet.*, **20**, 2263–2272.
14. Nikolova,E.N. *et al.* (2011) Transient Hoogsteen base pairs in canonical duplex DNA. *Nature*, **470**, 498–502.
15. Kitayner,M. *et al.* (2010) Diversity in DNA recognition by p53 revealed by crystal structures with Hoogsteen base pairs. *Nat. Struct. Mol. Biol*., **17**, 423–429.
16. Chen,Y. *et al.* (2010) Crystal structure of the p53 core domain bound to a full consensus site as a self-assembled tetramer. *Structure*, **18**, 246–256.
17. Kypr,J. *et al.* (2009) Circular dichroism and conformational polymorphism of DNA. *Nucleic Acids Res*., **37**, 1713–1725.
18. Ivanov,V.I. *et al.* (1974) The B to A transition of DNA in solution. *J. Mol. Biol*., **87**, 817–833.
19. Vorl□kov□M. *et al.* (1982) Conformational transitions of poly(dA-dT) poly(dA-dT) in ethanolic solutions. *Nucleic Acids Res*., **10**, 6969–6979.
20. Sutherland,J.C. *et al.* (1981) Z-DNA: vacuum ultraviolet circular dichroism. *Proc. Natl Acad. Sci. USA*, **78**, 4801–4804.
21. Sullivan,S.T. *et al.* (2001) A rare example of three abundant conformers in one retro model of the cisplatin-DNA d(GpG) intrastrand cross link. Unambiguous evidence that guanine O6 to carrier amine ligand hydrogen bonding is not important. possible effect of the Lippard base pair step adjacent to the lesion on carrier ligand hydrogen bonding in DNA adducts. *J. Am. Chem. Soc*., **123**, 9345–9355.
22. Tsankov,D. *et al.* (2003) Cisplatin adducts of d(CCTCTG*G*TCTCC).d(G GAGACCAGAGG) in aqueous solution by vibrational circular dichroism spectroscopy. *Biopolymers*, **72**, 490–499.
23. Takahara,P.M. *et al.* (1995) Crystal structure of double-stranded DNA containing the major adduct of the anticancer drug cisplatin. *Nature*, **377**, 649–652.
24. Andrushchenko,V. *et al.* (2007) DNA oligonucleotide-cis-platin binding: Ab initio interpretation of the vibrational spectra. *J. Phys. Chem. A*, **111**, 9714–9723.
25. Shepherd,J.H. (1989) Revised FIGO staging for gynaecological cancer. *Br. J. Obstet. Gynaecol*., **96**, 889–892.
26. Scully,R. *et al.* (1999) *Histological Typing of Ovarian Tumors*. Springer, Berlin, NY.
27. Lu,L. *et al.* (2012) Functional study of risk loci of stem cell-associated gene lin-28B and associations with disease survival outcomes in epithelial ovarian cancer. *Carcinogenesis*, **33**, 2119–2125.
28. Brewood,G.P. *et al.* (2008) A structural transition in duplex DNA induced by ethylene glycol. *J. Phys. Chem. B*, **112**, 13367–13380.
29. Wan,X. *et al.* (2002) Effect of insulin-like growth factor II on protecting myoblast cells against cisplatin-induced apoptosis through p70 S6 kinase pathway. *Neoplasia*, **4**, 400–408.
30. Ogawa,T. *et al.* (2010) Upregulation of IGF2 is associated with an acquired resistance for cis-diamminedichloroplatinum in human head and neck squamous cell carcinoma. *Eur. Arch. Otorhinolaryngol*., **267**, 1599–1606.
31. Lund,P. *et al.* (2004) Autocrine inhibition of chemotherapy response in human liver tumor cells by insulin-like growth factor-II. *Cancer Lett*., **206**, 85–96.

32. Krishna,A.G. *et al.* (1998) Taxol-DNA interactions: fluorescence and CD studies of DNA groove binding properties of taxol. *Biochim. Biophys. Acta*, **1381**, 104–112.
33. Malonga,H. *et al.* (2005) Taxol anticancer activity and DNA binding. *Mini Rev. Med. Chem*., **5**, 307–311.
34. Ouameur,A.A. *et al.* (2004) Taxol interaction with DNA and RNA - stability and structure features. *Candian J. Chem.*, **82**, 1112–1118.
35. Zhao,C. *et al.* (2012) Contrasting enantioselective DNA preference: chiral helical macrocyclic lanthanide complex binding to DNA. *Nucleic Acids Res*., **40**, 8186–8196.
36. Poklar,N. *et al.* (1996) Influence of cisplatin intrastrand crosslinking on the conformation, thermal stability, and energetics of a 20-mer DNA duplex. *Proc. Natl Acad. Sci. USA*, **93**, 7606–7611.
37. Kostrhunova,H. *et al.* (2000) Conformational analysis of site-specific DNA cross-links of cisplatin-distamycin conjugates. *Biochemistry*, **39**, 12639–12649.
38. Kim,S. *et al.* (2013) Probing allostery through DNA. *Science*, **339**, 816–819.
39. Huang,R.S. *et al.* (2011) Platinum sensitivity-related germline polymorphism discovered via a cell-based approach and analysis of its association with outcome in ovarian cancer patients. *Clin. Cancer Res.*, **17**, 5490–5500. *Received March 27, 2013; revised April 29, 2013; accepted May 10, 2013*

Table I. Associations of IGF-II rs4320932 genotype with clinical and pathological variables in epithelial ovarian cancer

Variable	*N*	TT	TC	CC	*P* value
		n (%)	*n* (%)	*n* (%)	
Stage					0.334
I–II	64	37 (57.8)	25 (39.1)	2 (3.1)	
III–IV	147	87 (59.2)	48 (32.7)	12 (8.2)	
P_{trend}				0.692	
Grade					0.703
1	34	22 (64.7)	11 (32.4)	1 (2.9)	
2	40	21 (52.5)	17 (42.5)	2 (5.0)	
3	137	81 (59.1)	45 (32.9)	11 (8.0)	
Histological type					0.279
Non-serous	126	74 (58.7)	41 (32.5)	11 (8.7)	
Serous	85	50 (58.8)	32 (37.7)	3 (3.5)	
P_{trend}				0.542	
Debulking result					0.374
Optimal (≤1 cm)	108	67 (62.0)	36 (33.3)	5 (4.6)	
Suboptimal (>1 cm)	100	55 (55.0)	36 (36.0)	9 (9.0)	
P_{trend}				0.185	
Residual tumor size					0.521
0	91	55 (60.4)	32 (35.2)	4 (4.4)	
>0	116	66 (56.9)	40 (34.5)	10 (8.6)	
P_{trend}				0.371	
Response to chemotherapy					**0.012**
Not complete	48	25 (52.0)	15 (31.3)	8 (16.7)	
Complete	128	79 (61.7)	45 (35.2)	4 (3.1)	
P_{trend}				**0.028**	

Table II. Associations of IGF-II rs4320932 genotype with patient survival outcomes in epithelial ovarian cancer

Genotype	Death			Progression		
	Events/*N*	Adj-HR	95% CI	Events/*N*	Adj-HR	95% CI
TT	48/120	1.00		47/120	1.00	
TC	33/71	1.48	0.94–2.34	39/71	**1.76**	**1.14–2.71**
CC	11/13	**3.28**	**1.64–6.57**	9/13	**3.05**	**1.47–6.37**
TC/CC	44/84	**1.74**	**1.15–2.65**	48/84	**1.92**	**1.28–2.88**
P_{trend}			**0.001**			**0.0004**

Adj-HR with patient age at surgery, disease stage, tumor grade, residual tumor size and histologic type. Events/*N*, events/total number.

Table III. Associations of IGF-II rs4320932 genotype with IGF phenotypes in epithelial ovarian cancer tissue

IGF expression	TT			TC			CC			*P* value
	N	Median	Range (5th–95th percentile)	*N*	Median	Range (5th–95th percentile)	*N*	Median	Range (5th–95th percentile)	
IGF-II mRNA	118	13.08	0–3008	71	8.78	0–9503	14	12.69	0–5661	0.980
IGF-II P1 mRNA	116	1.18	0–710	70	1.06	0–202	12	1.75	0–1544	0.600
IGF-II P2 mRNA	116	0.36	0–693	70	0.40	0–131	12	0	0–241	0.510
IGF-II P3 mRNA	116	198.70	0–31926	70	222.50	0–42127	12	448.38	8.57–4094	0.752
IGF-II P4 mRNA	116	48.16	0.13–1986	70	35.35	0.20–2075	12	40.22	0–2491	0.907
IGF-II peptide	123	95.03	30.9–435	73	99.20	23.86–438	14	87.41	34.4–517	0.790

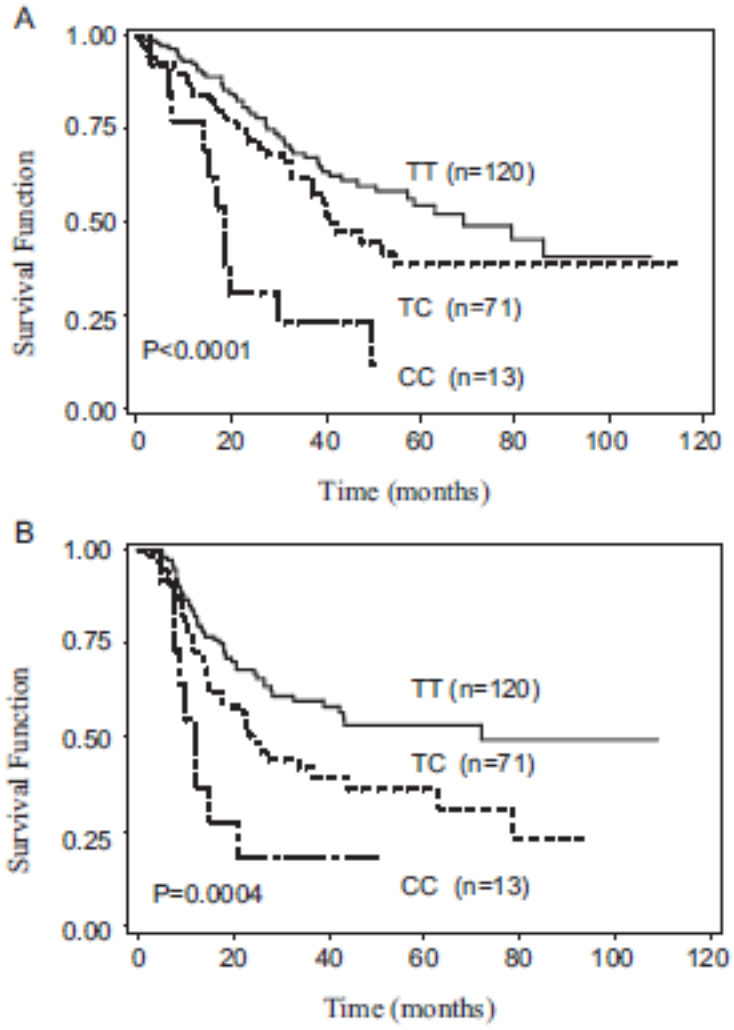

Fig. 1. Kaplan–Meier survival curves stratified by IGF-II genotype at rs4320932 in epithelial ovarian cancer. (**A**) Patients with the wild-type TT genotype exhibited superior overall survival; (**B**) Patients with the wild-type TT genotype exhibited superior progression-free survival.

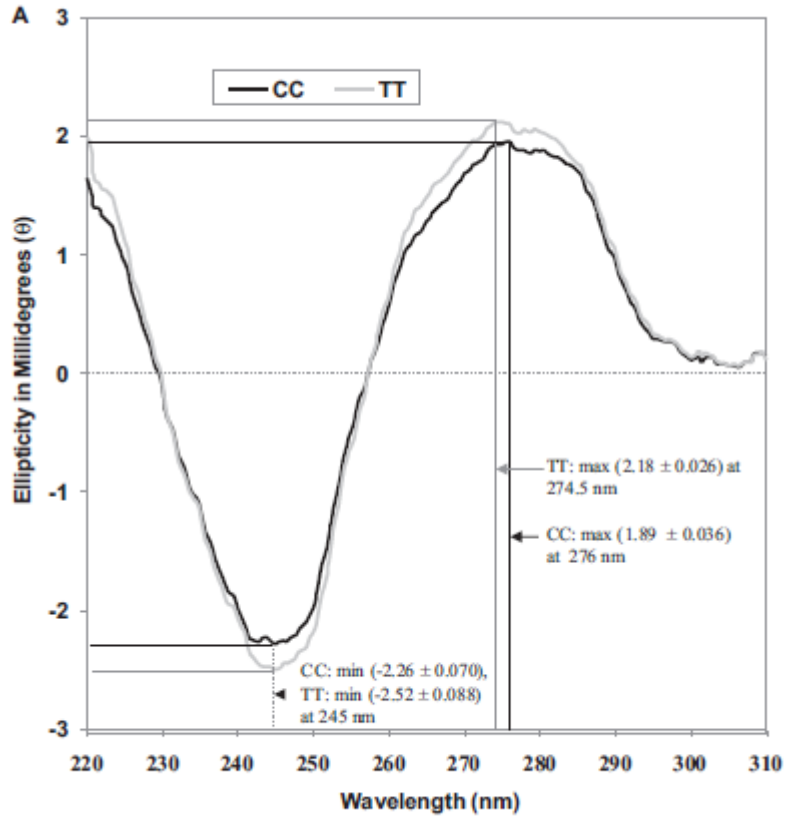
A
CC
TT
Ellipticity in Millidegrees (θ)
Wavelength (nm)
TT: max (2.18 ± 0.026) at 274.5 nm
CC: max (1.89 ± 0.036) at 276 nm
CC: min (-2.26 ± 0.070), TT: min (-2.52 ± 0.088) at 245 nm

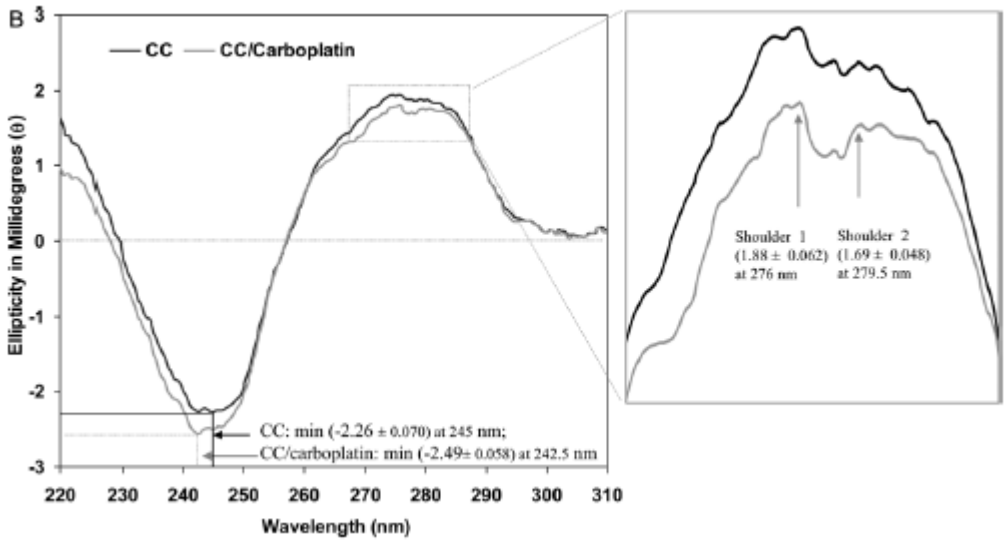
B
CC
CC/Carboplatin
Ellipticity in Millidegrees (θ)
Wavelength (nm)
CC: min (-2.26 ± 0.070) at 245 nm;
CC/carboplatin: min (-2.49± 0.058) at 242.5 nm
Shoulder 1 (1.88 ± 0.062) at 276 nm
Shoulder 2 (1.69 ± 0.048) at 279.5 nm

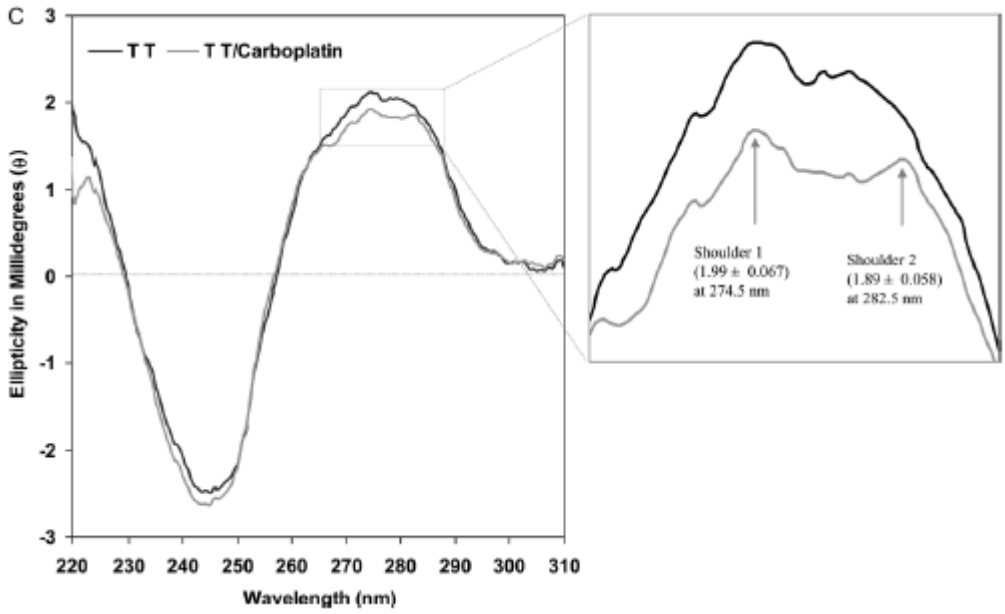
C
T T
T T/Carboplatin
Ellipticity in Millidegrees (θ)
3
2
1
0
-1
-2
-3
220
230
240
250
260
270
280
290
300
310
Wavelength (nm)
Shoulder 1
(1.99 ± 0.067)
at 274.5 nm
Shoulder 2
(1.89 ± 0.058)
at 282.5 nm